

March 01, 1992

The measurement of magnetostriction constants of thin films using planar microwave devices and ferromagnetic resonance

S. E. Bushnell
Northeastern University

W. B. Nowak
Northeastern University

S. A. Oliver
Northeastern University

C. Vittoria
Northeastern University

Recommended Citation

Bushnell, S. E.; Nowak, W. B.; Oliver, S. A.; and Vittoria, C., "The measurement of magnetostriction constants of thin films using planar microwave devices and ferromagnetic resonance" (1992). *Mechanical and Industrial Engineering Faculty Publications*. Paper 35.
<http://hdl.handle.net/2047/d20000726>

The measurement of magnetostriction constants of thin films using planar microwave devices and ferromagnetic resonance

S. E. Bushnell, W. B. Nowak,^{a)} S. A. Oliver,^{b)} and C. Vittoria
Department of Electrical and Computer Engineering, Northeastern University, Boston,
Massachusetts 02115

(Received 9 October 1991; accepted for publication 26 November 1991)

In this paper we introduce a new technique for measuring the saturation magnetostriction constant (λ_s) for isotropic polycrystalline thin films. The technique makes use of nonresonant planar microwave structures together with a novel stressing mechanism to induce a shift in the resonant field of a magnetic thin film as measured by a ferromagnetic resonance (FMR) experiment. Measurement of the shift induced by a uniaxial stress allows for determination of λ_s via a magnetic resonance analysis. Either a slotline device or coplanar waveguide (CPW) was used as the source of the microwave excitation field depending upon the orientation of the dc magnetic field. To evaluate the technique, polycrystalline Ni films of thickness of 637 nm were sputtered onto glass substrates at room temperature for comparison with the literature. Using a 50- Ω CPW, FMR measurements at 9 GHz revealed an average value of λ_s of -36×10^{-6} a value in agreement with those previously reported. The technique provides increased flexibility over other FRM techniques as it is wideband and directly accessible.

I. INTRODUCTION

Measurement of the saturation magnetostriction constant (λ_s) for thin films has been accomplished by a variety of techniques. The majority of these involve the accurate measurement of small displacements of a film (deposited onto a substrate), induced by a dc magnetic field (H) applied either in the plane or perpendicular to the film surface. Measurement of the deflection is accomplished by either using the film/substrate as part of a capacitance bridge,¹ use of an optical displacement meter,² or laser techniques.^{3,4}

Techniques for measuring λ_s using ferromagnetic resonance (FMR) have involved a variety of approaches,⁵⁻⁹ which in general include applying a stress to a material and measuring the resulting shift in the resonant dc field (H_r). Although the concept of measuring the shift in H_r to determine λ_s (for fixed frequency experiments) has been known and applied for some time,^{10,11} our technique differs from previous work in that it uses either a coplanar waveguide (CPW) or slotline device as the source for the microwave magnetic field (h_{rf}). This allows for localized application of h_{rf} (on the order of 0.5 mm or less for the CPW, transverse to the center conductor), measurements over a wide frequency range (0.1 GHz) $\leq f \leq$ 20 GHz, and a planar geometry that allows for simple access to the stressing assembly. The stressing assembly used here differs from others in that it utilizes a new type of beam support that eliminates the need for a clamped end.

II. ANALYSIS

A. Resonance conditions

The strong absorption of microwave energy by a ferromagnetic specimen due to the uniform precession of the

magnetic moments in an externally applied magnetic field is commonly termed FMR. The magnetic field value (H_r) corresponding to the FMR resonance, for a fixed microwave frequency, is strongly dependent upon the specimens magnetic parameters. This includes knowledge of the sample demagnetizing and anisotropy fields, their orientation with respect to the specimen magnetization (M), and the externally applied dc magnetic field. For isotropic polycrystalline thin films the experimentally deduced uniaxial anisotropy fields also need to be considered.

Calculation of the FMR resonance condition follows the method of Smit and Beljer's.¹² For a thin film having the coordinates shown in Fig. 1, the magnetic free energy of the system may be written as

$$F = -\mathbf{M} \cdot \mathbf{H} + \frac{1}{2} N_z M_z^2 - K_u^{\perp} \cos^2 \theta - K_u^{\parallel} \cos^2 \psi + \frac{3}{2} \lambda_s \tau \sin^2 \chi, \quad (1)$$

where K_u^{\perp} and K_u^{\parallel} are the uniaxial magnetic anisotropy parameters for the easy axis perpendicular and parallel to the film plane, respectively. The first two terms in Eq. (1) represent the Zeeman and demagnetizing energies, respectively. In addition, the magnetic energy due to uniaxial anisotropy is included through K_u^{\perp} and K_u^{\parallel} . Of most importance to this work is the addition of a stress (τ) dependent term in the free energy, $(3/2)\lambda_s\tau\sin^2\chi$, where λ_s is the saturation magnetostriction constant.¹³ The contribution of this term to the FMR resonance condition allows for the experimental evaluation of λ_s .

The FMR resonant condition is found from¹²

$$\frac{\omega^2}{\gamma^2} = \frac{1}{M^2 \sin^2 \theta} \left[\frac{\partial^2 F}{\partial \theta^2} \frac{\partial^2 F}{\partial \phi^2} - \left(\frac{\partial^2 F}{\partial \theta \partial \phi} \right)^2 \right], \quad (2)$$

subject to the additional constraints $\partial F / \partial \theta = 0$ and $\partial F / \partial \phi = 0$, and where γ is the gyromagnetic ratio. For the experimental condition where H is applied along the y axis, the resonance condition has the form

^{a)}Department of Mechanical Engineering, Northeastern University.

^{b)}Center for Electromagnetics Research, Northeastern University.

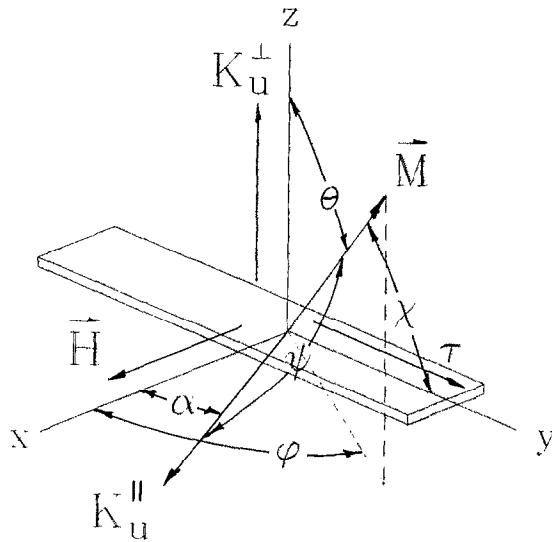


FIG. 1. Coordinate system used for magnetic free-energy analysis.

$$\frac{\omega^2}{\gamma^2} = [H_r + N_z M - H_a^{\perp} + H_a^{\parallel} \cos^2(\pi/2 - \alpha) + 3\tau\lambda_s/M] [H_r + H_a^{\parallel} \cos 2(\pi/2 - \alpha) + 3\tau\lambda_s/M], \quad (3)$$

where $H_a^{\perp} = 2K_u^{\perp}/M$, $H_a^{\parallel} = 2K_u^{\parallel}/M$, and the equilibrium position of M is assumed to be collinear with H . Since the microwave frequency is fixed, the effect of changes in the applied stress will result in a shift in the resonant magnetic field. By evaluating the partial differentials of Eq. (3) with respect to τ and H_r , the shift equation becomes

$$\frac{\Delta H_r}{\Delta \tau} = \frac{-3\lambda_s}{M}. \quad (4)$$

Similarly, when H is applied along the x direction, the resonance condition has the form

$$\frac{\omega^2}{\gamma^2} = [H_r + N_z M - H_a^{\perp} + H_a^{\parallel} \cos^2(\alpha)] \times [H_r + H_a^{\parallel} \cos 2(\alpha) - 3\tau\lambda_s/M], \quad (5)$$

where the equilibrium position of M is at $\theta = \pi/2$ and $\phi = 0$. The relation between the shift in the resonant field and applied stress is now more complex and is given by

$$\frac{\Delta H_r}{\Delta \tau} = \frac{3\lambda_s}{M} \frac{[H_r + N_z M - H_a^{\perp} + H_a^{\parallel} \cos^2(\alpha)]}{\{2H_r + N_z M - H_a^{\perp} + H_a^{\parallel} [3 \cos^2(\alpha) - 1]\}}, \quad (6)$$

where

$$|\{2H_r + N_z M - H_a^{\perp} + H_a^{\parallel} [3 \cos^2(\alpha) - 1]\}| \gg |3\tau\lambda_s/M|. \quad (7)$$

The magnetostriction constant may be experimentally derived through the use of Eqs. (4) and (6). The use of either (4) or (6) depends upon whether a slot or CPW

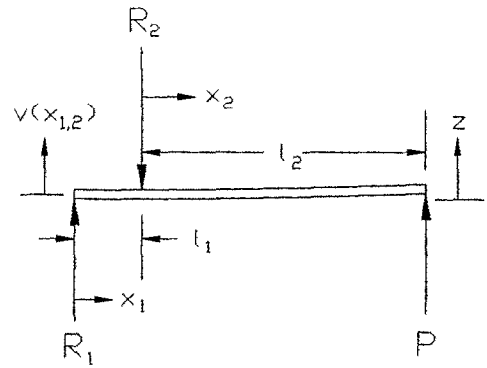


FIG. 2. Free-body diagram showing forces acting on the substrate. Simple supports are located at R_1 and R_2 .

device is used as the source for rf excitation of the film. As H must be perpendicular to h_{rf} in order to maximize absorption by the material, it must be oriented along the y and x axis for the slot and CPW devices, respectively. As discussed below, this is because h_{rf} is oriented parallel to the slot and transverse to the center conductor on the slot-line and CPW devices, respectively.

B. Stress calculations

Both Eqs. (4) and (6) rely on the accurate prediction of the change in stress in order to evaluate λ_s . Figure 2 depicts the free-body diagram for the substrate. The substrate was analyzed as a simply supported beam with distance l_1 between the two simple supports and l_2 between the center support and the applied load P . Using the shear and bending moments diagrams for the beam, in connection with the boundary conditions $v(x_1 = 0) = v(x_2 = 0) = 0$, $v(x_2 = l_2) = z$, and $dv/dx_1 = dv/dx_2$ at $x_1 = l_1$ and $x_2 = 0$, respectively, the deflections for the first and second sections of the beam may be expressed as

$$v(x_1) = \frac{1}{E_s I} \left(\frac{R_1 x_1^3}{6} - \frac{R_1 l_1^2 x_1}{6} \right), \quad 0 \leq x_1 \leq l_1 \quad (8)$$

and

$$v(x_2) = \frac{1}{E_s I} \left(\frac{-P x_2^3}{6} + \frac{R_1 l_1 x_2^2}{2} + \frac{R_1 l_1^2 x_2}{3} \right), \quad 0 \leq x_2 \leq l_2, \quad (9)$$

where E_s is the elastic modulus for the substrate, I is the area moment of inertia for the substrate, and P , R_1 , and R_2 are the applied and reactive loads, respectively.

Using Eq. (9), where $v(l_2) = z$, the load required to deflect the specimen an amount z is

$$P = \frac{3E_s I z}{l_2^2 (l_2 + l_1)}. \quad (10)$$

For some location on the top surface of the beam ($0 \leq x_2 \leq l_2$), the tensile stress may be represented by the flexure formula

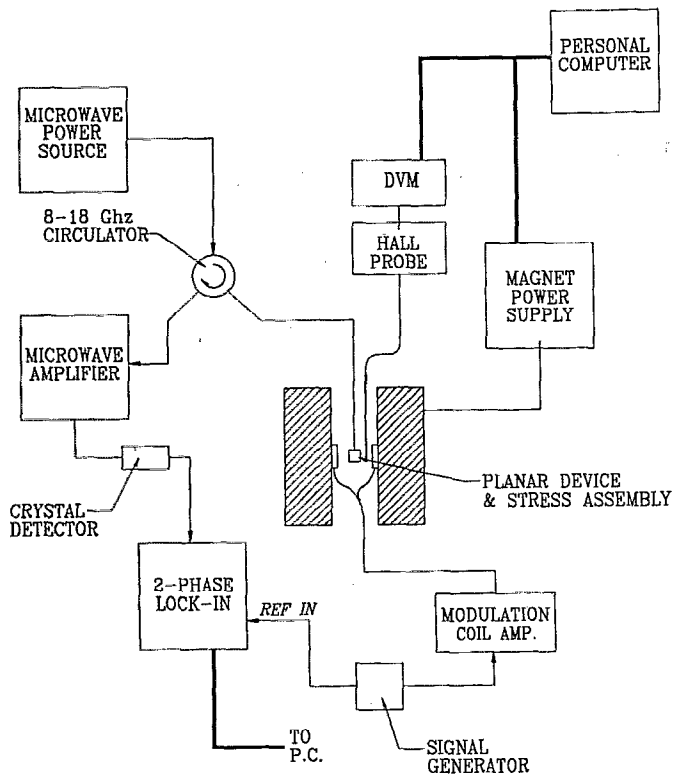


FIG. 3. Block diagram of the FMR experiment.

$$\tau_{yy} = \frac{M_b y}{I}, \quad (11)$$

where y is the distance from the neutral axis to the free surface M_b is the bending moment, and the shearing stresses $\tau_{yz} = \tau_{zy} = 0$. Using Eqs. (10) and (11) and Hooke's law, the strain along the top surface of the beam may be expressed as

$$\epsilon_{yy} = \frac{-3z(l_2 - x_2)(t/2)}{l_2^2(l_2 + l_1)}. \quad (12)$$

Finally, by assuming that the strain at the substrate/film interface is continuous, the stress in the film is simply

$$\tau_f = \epsilon_{yy} E_f, \quad (13)$$

where E_f is the elastic modulus of the film.

Evaluation of the stress in the film at some position x_2 requires only knowledge of the beam geometry, the elastic modulus of the film, and the deflection, z . Equations (12) and (13) are then combined with either Eq. (4) or (6) to obtain the magnetostriction constant.

III. EXPERIMENTS

Figure 3 shows a block diagram of the experiment. The experiment is designed to measure the derivative of the power reflected by the specimen as the magnetic field is swept through the FMR resonance. Microwave power from 0 to 10 mW is fed at a constant frequency to either the CPW or the slotline through an 8-18 GHz circulator. In addition to H , modulation coils apply a 1-kHz field to

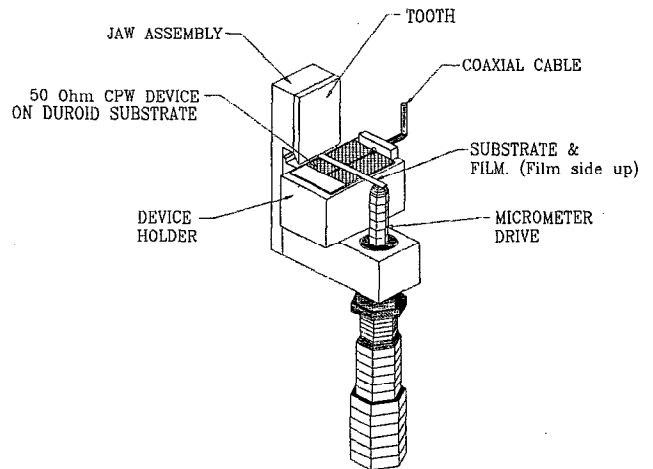


FIG. 4. Detail of the jaw assembly showing the locations of the substrate/film, planar device, and micrometer drive.

the specimen (collinear to H) ranging from 0 to 25 G. The signal generator used to drive the modulation coils also serves as an external reference to a two-phase lock-in. Once the signal is reflected from the specimen/device, it is amplified, detected, and entered into the lock-in, which extracts the 1-kHz component, which is proportional to the first derivative of the absorbed power with respect to H . The experiment is controlled via a personal computer which ramps the applied field, measures the field using a Hall probe/digital voltmeter interface, and collects the lock-in output.

The details of the stressing assembly are shown in Fig. 4. The geometry of the jaw assembly was chosen to eliminate the need for a clamped end which, upon being tightened, introduced stresses in the beam which were found to be nonuniform. After backing off the micrometer drive, the substrate/film was slid across the device surface until it touched the rear wall. The thin foot (0.76 mm wide) and tooth act as the simple supports in Fig. 2 at $x_1 = 0$ and $x_2 = 0$. Once in place, the tooth and micrometer drive were adjusted to allow approximately 0.25 mm clearance between the bottom of the substrate and the device plane. Experiments were conducted with the film away from the device (film side up) as this arrangement provided better signal-to-noise ratios due to the dielectric nature of the substrate. Once the substrate/film was in place, the micrometer was advanced 0.125 mm to remove any slack. Swept field tests were then conducted each time the drive

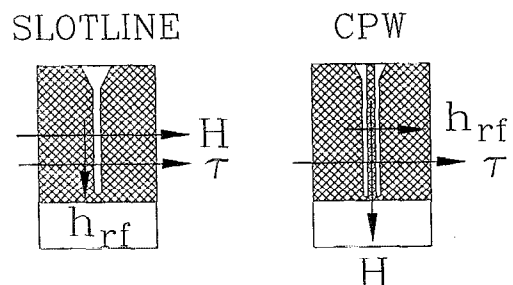


FIG. 5. Orientation of the microwave and dc magnetic fields, and stress for the slotline and CPW devices (top view).

was advanced, usually in increments of 0.025 or 0.05 mm.

The use of either the slotline or CPW device, and hence the use of Eqs. (4) or (6), is dependent primarily on the orientation of H . As shown in Fig. 5, the orientation of h_{rf} is parallel and perpendicular to the center slot and center conductor for the slotline and CPW, respectively.¹⁴ Thus, with H applied collinear to the stress, the slot and Eq. (4) are used to determine λ_p . For the case when H is perpendicular to τ , the CPW is used together with Eq. (6). To maximize the absorption in the specimen, the device holder could be moved relative to the jaw assembly assuring that the substrate/film rested over a position along the device wavelength that had maximum amplitude.

Both the CPW and slotline device were designed using closed-form expressions.¹⁴ The CPW was designed to match a coaxial line impedance of 50 Ω while the slot was designed for 75 Ω at 9 GHz. The slot was intentionally oversized due to the discrepancy between conventional design equations and experimental results.¹⁵ Dimensions for the CPW were as follows: the inner conductor width, s , was 0.38 mm and the two gaps, w_{CPW} were 0.16 mm each, bringing the total width between the ground planes to 0.70 mm. The slot width, w_s , was 0.195 mm. Both devices were constructed out of Duroid substrates ($\epsilon_r = 10.2$ and thickness $h = 0.635$ mm) and were shorted at the far end. Microwave power was coupled to the CPW using a standard 50- Ω connector with a 0.25-mm center conductor, while 2.16-mm coaxial cable (soldered to the device perpendicular to the slot) was used for the slotline.¹⁶

One of the benefits of the CPW device is the localized nature of h_{rf} , which curls around the center conductor. By keeping the total distance between the ground planes small, h_{rf} is similarly confined. The interaction volume in the material is therefore reduced and the resulting average of non-uniform stresses in the film is more accurate.

The limits of the deflection of the beam were fixed by the failure of the substrate. Typical maximum deflections for a substrate of 0.200 mm thick were 0.635 mm, a limit at which fracture would occur. Using Eqs. (12) and (13), where $E_f = 2.07 \times 10^{12}$ dyn/cm², the maximum stress applied to a film was 8.77×10^9 dyn/cm², corresponding to a 0.51-mm deflection. This stress is well within the elastic region of most transition metals.

IV. DISCUSSION

To evaluate the technique, Ni films were fabricated for test using ion-beam sputtering. The films were deposited on Dow Corning coverglasses (glass code 0211) using a 5-cm broad-beam source at 1.33×10^{-2} Pa of argon. The coverglasses were first cut from 4 \times 2-cm stock into 4-mm strips. Beam conditions of 1 keV and 100 mA/cm² were maintained throughout deposition after first evacuating and baking the chamber to a base vacuum of 6.66×10^{-6} Pa. Film thickness was measured to be 660 nm using a surface profilometer, including a Ge cap with an estimated thickness of 23 nm sputtered for corrosion resistance. Vibrating sample magnetometer (VSM) measurements taken on 5.6-mm diam disks established M at 488 G. As the

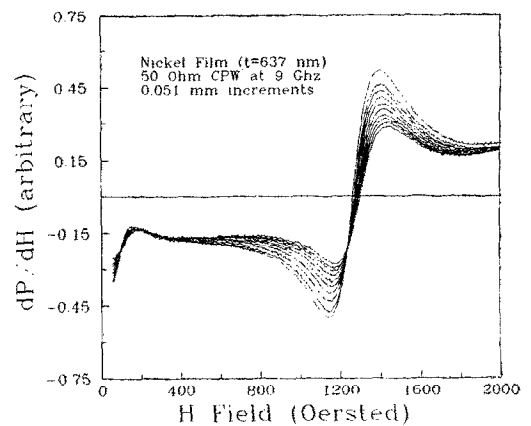


FIG. 6. FMR curves showing stress induced shift in H_r . Curves were collected every time the micrometer was advanced 0.051 mm.

substrates were not heated or cooled *in situ*, it is assumed that the films are polycrystalline with columnar grains.

Figure 6 shows a collection of resonance curves for a Ni thin film obtained while using a 50- Ω CPW and with H oriented along the x axis. Each curve was collected after advancing the micrometer 0.051 mm after initial adjustment of the substrate/film in the jaw assembly. The effect of stressing the film was to shift the resonant field to higher values (to the right). In addition, as the film was lifted further from the plane of the device the amplitude of the curves decreased simultaneously with the strength of h_{rf} . The result of both the shift in H_r and the reduction of the signal strength was the creation of a locus point below the zero crossing. The absorption at low fields may be due to domain wall motions.

Figure 7 shows the shift in H_r as a function of deflection of the free end. Values were established by curve fitting the linear region of each resonance curve (typically chosen as 30% of the linewidth), and using the first curve as a relative zero. By estimating the slope m and using

$$\frac{\Delta H_r}{\Delta \tau_f} = m \left(\frac{\Delta \tau_f}{\Delta z} \right)^{-1} \quad (14)$$

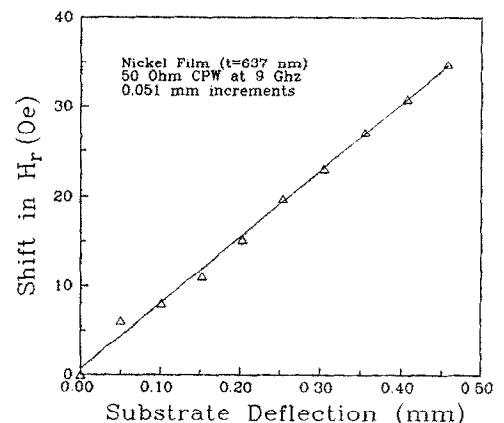


FIG. 7. Shift in H_r vs deflection of the substrate.

TABLE I. FMR runs on Ni films ($t = 637$ nm) and resulting values of λ_s .

Test ID	Device type	Frequency (GHz)	Avg. H_r (Oe)	Slope m (Oe/mm)	λ_s (10^6)
1	CPW	9.0	1300.6	75.1	-37
2	CPW	9.0	1279.2	73.9	-36
3	CPW	9.0	1277.1	68.0	-33
4	CPW	9.0	1282.0	74.7	-37

and Eq. (6), λ_s was calculated to be -36×10^{-6} where H_a^{\perp} and H_a^{\parallel} were assumed equal to zero, and $E_f = 2.07 \times 10^{12}$ dyn/cm². Table I summarizes other tests conducted using the 50- Ω CPW device. Rough tests were completed using a 75- Ω slot. Slopes of approximately -118 Oe/mm were observed, indicating the resonant shifts were of the right magnitude and correct direction.

The values of λ_s for Ni measured by this method compare well with those measured by other authors. Kloholm and Aboaf reported values of -38×10^{-6} .¹⁷ Aria *et al.* reported -30×10^{-6} using an optical displacement meter,⁴ and Kaneko *et al.* measured values of -30×10^{-6} using piezoelectric substrates.² Values for bulk isotropic polycrystalline Ni are predicted to be -33×10^{-6} using the relation

$$\lambda_s = \frac{2}{3}\lambda_{100} + \frac{1}{3}\lambda_{111}, \quad (15)$$

where $\lambda_{100} = -45.9 \times 10^{-6}$ and $\lambda_{111} = -24.3 \times 10^{-6}$.¹⁸

As discussed above, the lack of a single standard makes the absolute accuracy of the experiment difficult to establish. However, both the sensitivity and accuracy are influenced by a number of factors. First, the modulus of elasticity of the film must be estimated. For novel alloys, bulk values are often unpublished or unapplicable. Second, to achieve a sensitivity of 10^{-7} using the current beam geometry, shifts in H_r of 10^{-2} G must be measured routinely. At present, a variety of experimental parameters make this difficult. Although increasing the thickness of the substrate improves the gain of the experiment (by increasing the stress), the substrate must be located with the film side flipped down towards the device plane. With the film side down, coupling between the metal film and the device changed the reflected power as the film/substrate was deflected. To obtain a stable power level using this

configuration an appropriate frequency had to be found.

Although FMR has been used to evaluate λ_s by other means, to the best of our knowledge this is the first method that uses planar-type devices (together with a simple stressing mechanism) that allows for easy determination of λ_s . The technique should be useful for any thin magnetic film fabrication process. While the use of the slotline device is preferable to the CPW for materials with large uniaxial anisotropies, the CPW allows for localized excitation of the specimen. As the method is based upon FMR techniques, it also yields estimates of line width and with modifications could provide anisotropy constants. Finally, the sensitivity of the technique is more than adequate to make the approach a simple technique for evaluating materials with large and small magnetostriction constants.

ACKNOWLEDGMENTS

We would like to extend our gratitude to Don S. Rodbell for his advice and consultations regarding several aspects of this project and the Rogers Corporation for providing the Duroid substrates.

- ¹E. Kloholm, IEEE Trans. Magn. MAG-12, 819 (1976).
- ²M. Kaneko, S. Hashimoto, M. Hayakawa, and K. Aso, J. Phys. E 21, 487 (1988).
- ³A. C. Tam and H. Schroeder, J. Appl. Phys. 64, 5422 (1988).
- ⁴K. I. Arai, M. Yamaguchi, and C. S. Muranaka, IEEE Trans. Magn. 25, 4201 (1989).
- ⁵B. Hoekstra, F. van Doveren, and J. M. Robertson, Appl. Phys. 12, 261 (1977).
- ⁶J. C. M. Henning and J. H. den Boef, Appl. Phys. 16, 353 (1978).
- ⁷G. P. Vella-Coleiro, Rev. Sci. Instrum. 50, 1130 (1979).
- ⁸X. Wang, C. S. Kraft, and M. H. Kryder, IEEE Trans. Magn. MAG-18, 1295 (1982).
- ⁹L. Pust and Z. Frait, Phys. Status Solidi A 85, 179 (1984).
- ¹⁰A. B. Smith and R. V. Jones, J. Appl. Phys. 34, 1283 (1963).
- ¹¹A. B. Smith, Rev. Sci. Instrum. 39, 378 (1968).
- ¹²J. Smit and H. G. Beljers, Philips Res. Rep. 10, 113 (1955).
- ¹³C. Kittel, Rev. Mod. Phys. 21, 541 (1949).
- ¹⁴K. C. Gupta, *Microstrip Lines and Slotlines* (Artech House, Dedham, MA, 1979), pp. 215 and 275.
- ¹⁵E. Mariani, C. Heinzman, J. Agrios, and S. Cohn, IEEE Trans. Microwave Theory Tech. MTT-17, 1091 (1969).
- ¹⁶G. H. Robinson and J. L. Allen, IEEE Trans. Microwave Theory Tech. MTT-17, 1097 (1969).
- ¹⁷E. Kloholm and J. Aboaf, J. Appl. Phys. 53, 2661 (1982).
- ¹⁸Sushin Chikazumi, *Physics of Magnetism* (Krieger, Malabar, FL, 1964), p. 173.

Review of Scientific Instruments is copyrighted by the American Institute of Physics (AIP). Redistribution of journal material is subject to the AIP online journal license and/or AIP copyright. For more information, see <http://ojps.aip.org/rsio/rsicr.jsp>
Copyright of Review of Scientific Instruments is the property of American Institute of Physics and its content may not be copied or emailed to multiple sites or posted to a listserv without the copyright holder's express written permission. However, users may print, download, or email articles for individual use.